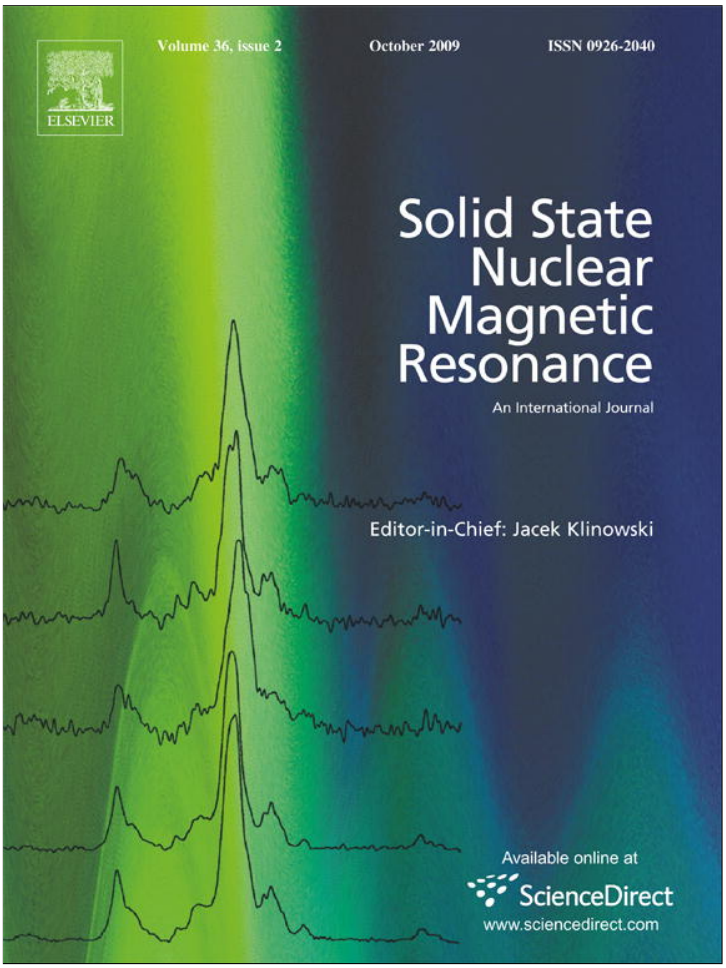

Solid State Nuclear Magnetic Resonance 36 (2009) 77–85

Contents lists available at ScienceDirect

Solid State Nuclear Magnetic Resonance

journal homepage: www.elsevier.com/locate/ssnmr

NMR dipolar constants of motion in liquid crystals: Jeener–Broekaert, double quantum coherence experiments and numerical calculation on a 10-spin cluster

H.H. Segnorile, C.J. Bonin, C.E. González, R.H. Acosta, R.C. Zamar *

Facultad de Matemática, Astronomía y Física, Universidad Nacional de Córdoba - IFFaMAF M. Allende y H. de la Torre - Ciudad Universitaria, X5016LAE - Córdoba, Argentina

ARTICLE INFO

Article history:
Received 28 January 2009
Received in revised form
8 June 2009
Available online 21 June 2009

Keywords:
Dipolar order
Multiple quantum coherence
Spin dynamics
Quasi-equilibrium states

ABSTRACT

Two proton quasi-equilibrium states were previously observed in nematic liquid crystals, namely the $\mathscr{S}$ and $\mathscr{W}$ quasi-invariants. Even though the experimental evidence suggested that they originate in a partition of the spin dipolar energy into a strong and a weak part, respectively, from a theoretical viewpoint, the existence of an appropriate energy scale which allows such energy separation remains to be confirmed and a representation of the quasi-invariants is still to be given. We compare the dipolar NMR signals yielded both by the Jeener–Broekaert (JB) experiment as a function of the preparation time and the free evolution of the double quantum coherence (DQC) spectra excited from the $\mathscr{S}$ state, with numerical calculations carried out from first principles under different models for the dipolar quasi-invariants, in a 10-spin cluster which represents the 5CB (4′-pentyl-4-biphenyl-carbonitrile) molecule. The calculated signals qualitatively agree with the experiments and the DQC spectra as a function of the single-quantum detection time are sensible enough to the different models to allow both to probe the physical nature of the initial dipolar-ordered state and to assign a subset of dipolar interactions to each constant of motion, which are compatible with the experiments. As a criterion for selecting a suitable quasi-equilibrium model of the 5CB molecule, we impose on the time evolution operator consistency with the occurrence of two dipolar quasi-invariants, that is, the calculated spectra must be unaffected by truncation of non-secular terms of the weaker dipolar energy. We find that defining the $\mathscr{S}$ quasi-invariant as the subset of the dipolar interactions of each proton with its two nearest neighbours yields a realistic characterization of the dipolar constants of motion in 5CB. We conclude that the proton-spin system of the 5CB molecule admits a partition of the dipolar energy into a bilinear strong and a multiple-spin weak contributions therefore providing two orthogonal constants of motion, which can be prepared and observed by means of the JB experiment. This feature, which implies the existence of two timescales of very different nature in the proton-spin dynamics, is ultimately dictated by the topology of the spin distribution in the dipole network and can be expected in other liquid crystals. Knowledge of the nature of the dipolar quasi-invariants will be useful in studies of dipolar-order relaxation, decoherence and multiple quantum NMR experiments where the initial state is a dipolar-ordered one.

1. Introduction

Nuclear spin dipolar quasi-invariants are, together with the Zeeman energy, relevant observables of the spin system in liquid crystals (LC), providing new relaxation parameters useful to disentangle the complex molecular motions in these mesophases [1]. For instance, Larmor frequency and temperature dependent experiments showed that the relaxation times of the dipolar quasi-invariants are very sensitive to slow cooperative molecular motions over a wide range of magnetic field strengths, allowing to reliably estimate the spectral densities of the nematic director [2,3]. However, nowadays, difficulties associated with the theoretical description still remain, which hamper taking full advantage of the useful relaxation properties of the dipolar-ordered states [4].

A comprehensive theoretical description of the spin dynamics in the relaxation or the decoherence regime in highly correlated molecular systems must include both the quantum correlation between spins and environment in the microscopic timescale together with a description of the physical processes which drive the spin system to the quasi-equilibrium [3–6]. However, any further theoretical progress depends on a suitable representation of the dipolar quasi-invariants. This requirement also applies to manipulation of quantum states starting from dipolar-ordered

* Corresponding author.
E-mail address: zamar@famaf.unc.edu.ar (R.C. Zamar).

0926-2040/$ - see front matter © 2009 Elsevier Inc. All rights reserved.
doi:10.1016/j.ssnmr.2009.06.003

states in LC, as in multiple quantum NMR experiments [7–9]. In this work, we attempt to provide physical insight on the origin of different thermodynamic quasi-invariants and their multiple-spin nature by comparing the output of different NMR experiments with the corresponding signals calculated from first principles.

The feasibility of preparing nuclear spin dipolar-ordered states in solids has been established in the past [10–12]. One of the best known methods for generating dipolar order from Zeeman order is the Jeener–Broekaert (JB) phase-shifted radiofrequency (rf) pulse pair [12]. In ordinary solids, as CaF_2, where the nuclear spins are regularly distributed, the assembly of fluorines presents two independent quasi-invariants at high magnetic field: the Zeeman and secular dipolar energies [12]. The occurrence of these constants of motion relies on the fact that, at high magnetic field, the non-secular terms of the dipolar energy have negligible influence on the time evolution of the quantum coherences in the timescale of the build up of the quasi-equilibrium state. Recently, the tensor structure of the density matrix after the JB pulse pair during the transient towards the quasi-equilibrium has been studied by encoding its coherence numbers in a basis orthogonal to the Zeeman basis [7]. The only dipolar quasi-constant observed was the high-field secular dipolar Hamiltonian.

The proton-spin distribution in hydrated crystals presents a higher degree of complexity than ordinary solids, since protons are paired in water molecules throughout the crystal lattice [13–15]. Under an adequate orientation respect to the external magnetic field, all spin pairs are equivalent and the NMR spectrum shows a resolved doublet due to the "intrapair" interactions while the "interpair" contribution provides the crystalline broadening [15]. The spin system can be then assumed as an arrangement of weakly coupled equivalent pairs. Accordingly, the dipolar Hamiltonian is written in a perturbative way as a sum of two commuting contributions: an intrapair term and a smaller crystalline interpair contribution, the latter truncated with respect to the intrapair and Zeeman energies. Again in this case, it is assumed that the elimination of the non-secular terms of the interpair dipolar energy has no significant effect on the coherence time evolution during the build up of the thermal equilibrium. A Hamiltonian of this form is compatible with the occurrence of four quasi-invariants, three of them (Zeeman, dipolar intrapair, and singlet orders) associated with the unequally spaced energy levels of a proton pair, and the crystalline dipolar interpair. This assumption was experimentally corroborated in gypsum [15–17] and potassium oxalate monohydrate [14].

Liquid crystals provide another example of spin system where two kinds of independent proton-spin dipolar-ordered states can be prepared and observed at high magnetic fields. Dipolar signals similar to those of the hydrated crystals were observed in fully protonated and partially deuterated nematics at 300 MHz as well as 16 and 27 MHz [18,1]. It is accepted that the fast liquid-like molecular motion averages out the intermolecular dipolar interactions, however, there is a strong residual intramolecular dipolar spin energy due to the orientational order typical of these mesophases [19]. In this work we assume that, except for spin relaxation, a picture of magnetically isolated clusters of dipole coupled spins is adequate for representing the spin system in LC [20,21]. This characteristic enables studying the transfer of the high-field Zeeman order to dipolar order in small spin systems. The NMR lineshape of nematics is broad and often shows a resolved doublet (independent of the external field) which indicates that the interaction of a spin with its nearest neighbours is strong enough to establish a coherent response in spite of the broadening effects due to more distant spins [22,23].

The occurrence of two dipolar quasi-invariants in LC suggests that a perturbative approximation of the spin–spin Hamiltonian should hold, in which the high-field Zeeman-secular dipolar energy $\mathscr{H}_D^0$ is split in two commuting terms [1] associated with two subsets, strong ($\mathscr{S}$) and weak ($\mathscr{W}$), of dipolar couplings. However, the existence of an appropriate energy scale which justifies truncation of the weaker term to generate two constants of motion associated with the dipolar energy is not clearly suggested in LC as in hydrated solids, because of the very different nature of the dipolar network and the limited number of degrees of freedom of the LC molecule. By encoding the spin states after the JB pulse pair on the X-basis, it was recently shown [24] that $\mathscr{S}$ in 5CB (4′-pentyl-4-biphenyl-carbonitrile) has a bilinear pairwise tensor structure like $\mathscr{H}_D^0$, while $\mathscr{W}$ has a much more complex, multiple-spin correlated nature, in consistency with the longer timescale associated with this quasi-invariant [1]. However, this method does not allow finding the appropriate energy scale which justifies truncation of the weaker term to generate a second constant of motion associated with the dipolar energy.

In this work we explore the validity of representing the quasi-equilibrium spin states after the JB preparation pulse pair in LC by a density operator with two dipolar quasi-invariants originated in the intra-molecular Zeeman-secular dipolar energy, and propose a method for identifying a partition of the dipolar energy into two dipolar constants of motion. We study the experimental single- (SQC) and double quantum coherence (DQC) signals of 5CB, obtained from the initial $\mathscr{S}$ dipolar-ordered state, and compare them with the corresponding signals calculated through the exact quantum dynamics of a cluster of ten spins $\frac{1}{2}$ at the proton sites of a 5CB molecule.

The dipolar quantum operators are built by partitioning the secular dipolar energy and truncating the weak term with respect to the strong one. As the criterion for selecting an appropriate partition, we require the time evolution of the quantum coherence to be consistent with the occurrence of the $\mathscr{S}$ and $\mathscr{W}$ quasi-invariants, namely the NMR signals calculated under a satisfactory partition of the dipolar energy must be unaffected by neglecting the non-secular part of the weak dipolar energy in the common eigen-basis of the Zeeman and strong dipolar energy.

2. 5CB molecule and dipolar couplings

The 5CB molecule has 19 protons: eight at the benzene rings (core) and the others at the alkyl chain. In the numerical calculations carried out in this work, the spin system consists of the 10 labelled protons at the 5CB molecule sketched in Fig. 1. This is a thermotropic LC, extensively used in NMR investigations. Its nematic range is near room temperature which turns this compound suitable from a practical point of view. The molecular structure of 5CB, which is characteristic of many LC, allows examining the idea of a quasi-equilibrium state characterized by a single spin temperature, even in presence of protons having different environment and dynamics.

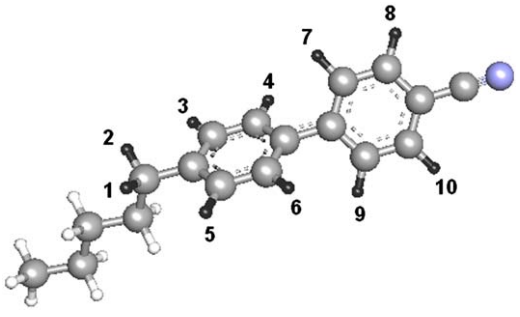

Fig. 1. Sketch of the 5CB (4′-pentyl-4-biphenyl-carbonitrile) molecule. Protons are numbered as used in the calculations.

The numerical calculations of this work demand the use of dipolar couplings between the interacting protons of our models, but only some of them are reported in the literature. In order to estimate the remaining couplings we use an average 5CB molecule with geometrical parameters obtained from Refs. [25,26]. Table 1 contains the dipolar couplings D_{ij} between protons i and j, as defined by Eq. (3). The dipolar couplings yielded by the average molecule agree, within experimental error, with those of the molecular core measured in Refs. [25,27] in $5CB_{d11}$ [28], except for D_{47} and D_{69} which are affected by internal molecular motions. In such case, we adopted the experimental values. For the same reason, we used the couplings calculated from the molecular dynamics trajectory in Ref. [26] for D_{15}, D_{23}, D_{16} and D_{24}. One can expect that internal molecular motion is not a strong perturbation to the dipolar couplings of distant protons like the ones we estimated from the average molecule. Then, the set of D_{ij} values of Table 1 stand for a 10-spin model for a representative 5CB molecule suitable for NMR calculations.

3. Theoretical approach

3.1. Background

The relevant Hamiltonian of a system of dipole-coupled like spins $\frac{1}{2}$ in a strong external magnetic field $\mathbf{B}_o$, in units of $\hbar$, is

$$\mathscr{H} = \mathscr{H}_Z + \mathscr{H}_D^o, \tag{1}$$

where the Zeeman energy $\mathscr{H}_Z = -\omega_o \mathbf{I}_z$, with ω_o the Larmor frequency, and

$$\mathscr{H}_D^o = \sqrt{6}\sum_{i<j} D_{ij}\mathbf{T}_{20}^{ij} \tag{2}$$

is the secular part of the dipole–dipole interaction (high-field approximation) and $\mathbf{T}_{20}^{ij} = (1/\sqrt{6})[2I_z^i I_z^j - \frac{1}{2}(I_+^i I_-^j + I_-^i I_+^j)]$. In LC

$$D_{ij} \equiv \left\langle \frac{\mu_o \gamma^2 \hbar}{4\pi}\left(\frac{1-3\cos^2\theta_{ij}}{2r_{ij}^3}\right)\right\rangle \tag{3}$$

is the dipolar coupling constant of nuclei i and j averaged over the molecular motion, r_{ij} is the distance between spins, θ_{ij} is the angle between the internuclear vector and the magnetic field and the sums run over protons within a molecule. Since we are interested in a time scale much shorter than any relaxation time, the dynamics of the spin system is represented by the Liouville–Von Neumann equation [29].

The pulse method for creating and detecting dipolar order in dipole-coupled spin systems at high magnetic fields, introduced by Jeener and Broekaert [12] consists of the phase-shifted radiofrequency pulses $90_x - t_1 - 45_y - t_2 - 45_y - t$ sketched in Fig. 2(a). The single-quantum coherences created by the first pulse evolve during t_1 mainly under the dipole spin–spin Hamiltonian (in the rotating frame). Along this period, multi-spin single-quantum coherences develop, and the second 45_y pulse transforms part of the coherences just created into multi-spin order [24,30–32]. Within a period of a few T_2^* (the characteristic decay time of the NMR signal), the subsystems attain states of internal quasi-equilibrium, which can be characterized by a spin temperature [33]. Over a much larger time scale, spin–lattice relaxation makes the dipolar and Zeeman temperatures to depend on time, until each subsystem reaches a state of thermal equilibrium with the lattice [4]. Finally, the third pulse converts the created order into observable single-quantum coherence.

3.2. Time evolution operator and the dipolar constants of motion

As pointed out in Section 1, there is experimental evidence that in LC two dipolar quasi-invariants can be prepared and observed independently at high magnetic fields [1,34]. It is convenient for later purposes to split the dipolar Hamiltonian of Eq. (2) into two parts, in order to account for the occurrence of two categories of dipolar couplings: strong and weak. Accordingly, we start by writing the dipolar Hamiltonian as

$$\mathscr{H}_D^o = \mathscr{H}_D^{o(\mathscr{S})} + \mathscr{H}_D^{o(\mathscr{W})}, \tag{4}$$

where both terms have the tensor structure of Eq. (2). $\mathscr{H}_D^{o(\mathscr{S})}$ involves the subset of the strong dipolar pairwise interactions within the molecule, namely

$$\mathscr{H}_D^{o(\mathscr{S})} = \sqrt{6}\sum_{i<j\in\mathscr{S}} D_{ij}\mathbf{T}_{20}^{ij}, \tag{5}$$

while

$$\mathscr{H}_D^{o(\mathscr{W})} = \sqrt{6}\sum_{i<j\in\mathscr{W}} D_{ij}\mathbf{T}_{20}^{ij} = \mathscr{H}_D^{o(\mathscr{W},\mathrm{d})} + \mathscr{H}_D^{o(\mathscr{W},\mathrm{nd})} \tag{6}$$

Table 1
Dipolar couplings of the core and α–CH_2 protons of the average 5CB molecule with $S_{zz} = 0.54$ corresponding to 27 °C.

i	j	D_{ij} (Hz)	i	j	D_{ij} (Hz)	i	j	D_{ij} (Hz)
1	2	5482.1	4	6	395.5	4	10	−120.2
5	6	−4477.9	7	9	395	5	7	−119.3
3	4	−4418.3	1	6	−383[a]	6	8	−119.3
7	8	−4396.8	2	4	−383[a]	2	5	100.5
9	10	−4391.5	2	7	−228.9	2	8	−90.6
4	7	−1741[b]	1	4	−212	5	8	−89.5
6	9	−1741[b]	2	6	−192.1	3	10	−89.4
1	5	−1121[a]	6	7	173	1	8	−76.9
2	3	−1121[a]	1	7	−170.7	4	5	74.7
3	7	−414.5	4	9	170.1	1	10	−74.6
6	10	−409.7	1	9	−161.3	8	9	72.4
4	8	−407.7	3	8	−156.8	3	6	71
5	9	−406.6	5	10	−156.3	7	10	70.8
3	5	401.9	2	9	−125.2	2	10	−65.4
8	10	399.8	3	9	−120.5	1	3	42

[a] Data from Ref. [26] (scaled with a factor of 1.15).
[b] From Refs. [25,27].

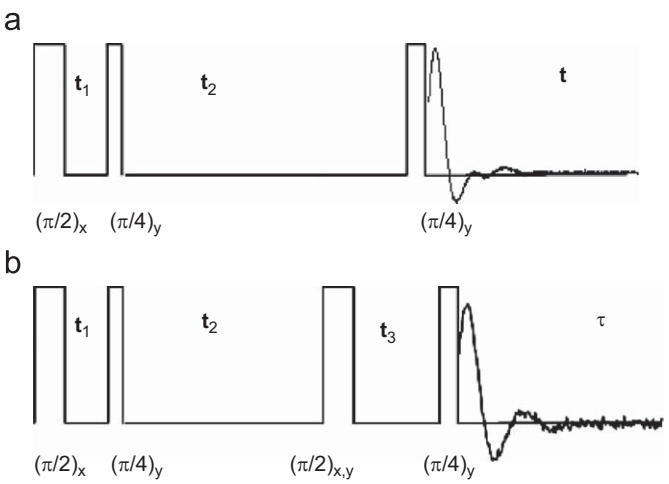

Fig. 2. (a) Jeener–Broekaert pulse sequence to generate dipolar order. The spin state after the second pulse evolves towards a quasi-equilibrium state over a time period of a few T_2^*. The single-quantum signal produced by the read pulse is a measure of the order created. (b) Sketch of the 4-pulse sequence used for selective excitation and detection of the DQC starting from the dipolar-ordered state. The first two pulses are the Jeener–Broekaert preparation pulses. The waiting time was set $t_2 = 2$ ms to allow the quasi-equilibrium to establish.

is the part of the dipolar energy which involves the weaker pairwise interactions. Superscripts "d" and "nd" mean diagonal and non-diagonal (in blocks) parts of the $\mathscr{W}$ dipolar energy with regard to $\mathscr{H}_Z$ and $\mathscr{H}_D^{o(\mathscr{S})}$. The occurrence of two dipolar constants of motion demands the norm of the operators to satisfy $\|\mathscr{H}_Z\| \gg \|\mathscr{H}_D^{o(\mathscr{S})}\| \gg \|\mathscr{H}_D^{o(\mathscr{W})}\|$, which justifies retaining only the truncated $\mathscr{H}_D^{o(\mathscr{W},\mathrm{d})}$ in the second equality of Eq. (6), in a perturbative view [14]. It is worth to notice that due to the truncation inherent in its definition, $\mathscr{H}_D^{o(\mathscr{W},\mathrm{d})}$ (and also $\mathscr{H}_D^{o(\mathscr{W},\mathrm{nd})}$) does not preserve the bilinear form of Eq. (2), and may have a much more complex structure [24].

An expression for $\mathscr{H}_D^{o(\mathscr{W},\mathrm{d})}$ in operator form is not available at present, except for the case of weakly coupled equivalent pairs [14]. The matrix representation of $\mathscr{H}_D^{o(\mathscr{W},\mathrm{d})}$, used in this work, is obtained by writing $\mathscr{H}_D^{o(\mathscr{W})}$ in the common eigen-basis of $\mathscr{H}_Z$ and $\mathscr{H}_D^{o(\mathscr{S})}$ (since $[\mathscr{H}_Z, \mathscr{H}_D^{o(\mathscr{S})}] = 0$), retaining only the diagonal blocks (diagonal blocks occur when degenerate eigen-values exist [35]). The remaining elements constitute $\mathscr{H}_D^{o(\mathscr{W},\mathrm{nd})}$. The Hamiltonians so defined satisfy the commutation relations

$$[\mathscr{H}_Z, \mathscr{H}_D^{o(\mathscr{W},\mathrm{d})}] = 0, \quad [\mathscr{H}_Z, \mathscr{H}_D^{o(\mathscr{W},\mathrm{nd})}] = 0, [\mathscr{H}_D^{o(\mathscr{S})}, \mathscr{H}_D^{o(\mathscr{W},\mathrm{d})}] = 0, \quad [\mathscr{H}_D^{o(\mathscr{S})}, \mathscr{H}_D^{o(\mathscr{W},\mathrm{nd})}] \neq 0, [\mathscr{H}_D^{o}, \mathscr{H}_D^{o(\mathscr{S})}] \neq 0, \tag{7}$$

and the orthogonality relations

$$\mathrm{Tr}\{\mathscr{H}_Z \mathscr{H}_D^{o(\mathscr{W},\mathrm{d})}\} = 0, \quad \mathrm{Tr}\{\mathscr{H}_Z \mathscr{H}_D^{o(\mathscr{S})}\} = 0, \quad \mathrm{Tr}\{\mathscr{H}_D^{o(\mathscr{S})} \mathscr{H}_D^{o(\mathscr{W},\mathrm{d})}\} = 0. \tag{8}$$

The dipolar Hamiltonian can be written in a condensed way as

$$\mathscr{H}_D^{o} = \mathscr{H}_{qe} + \mathscr{H}_D^{o(\mathscr{W},\mathrm{nd})}, \tag{9}$$

where

$$\mathscr{H}_{qe} \equiv \mathscr{H}_D^{o(\mathscr{S})} + \mathscr{H}_D^{o(\mathscr{W},\mathrm{d})} \tag{10}$$

is the part of the Hamiltonian spanned in quasi-invariants.

In the following we aim to classify the dipolar energy terms into strong and weak in consistency with the perturbation scheme in order to define the relevant observables. The choice of the interactions, which compose the subsets $\mathscr{S}$ and $\mathscr{W}$ of Eqs. (5) and (6), is not evident in LC due to the dispersion of the dipolar couplings within the molecule. We adopt the criterion that the two quasi-invariants are properly defined only if the time evolution of the spin state calculated with the whole Hamiltonian $\mathscr{H}_D^{o}$ is indistinguishable from that calculated with the truncated one, $\mathscr{H}_{qe}$. In this way we ensure that the diagonal part of the density operator of a quantum state, namely the part spanned in constants of motion, does not evolve in time while spin dynamics develops [see Eq. (15)]. In order to illustrate the validity of this criterion we first analyse the transient towards the quasi-equilibrium of the state ensuing the preparation pulses of the JB sequence.

The time evolution of the density operator under $\mathscr{H}_D^{o}$, at time t_2 after the second JB pulse is

$$\rho(t_1,t_2) = e^{-i(\mathscr{H}_{qe}+\mathscr{H}_D^{o(\mathscr{W},\mathrm{nd})})t_2}\rho(t_1,0)e^{i(\mathscr{H}_{qe}+\mathscr{H}_D^{o(\mathscr{W},\mathrm{nd})})t_2} = U_{nd}(t_2)e^{-i\mathscr{H}_{qe}t_2}\rho(t_1,0)e^{i\mathscr{H}_{qe}t_2}U_{nd}^{\dagger}(t_2), \tag{11}$$

where $\rho(t_1,0) \equiv \rho(t_1,t_2=0)$ is the density operator immediately after the second pulse, $U_{nd}(t) = T_-\exp\{-i\int_0^t \mathscr{H}_D^{o(\mathscr{W},\mathrm{nd})}(s)\,ds\}$ is a time-ordered exponential operator where operators are ordered from right to left as time decreases [36] and $\mathscr{H}_D^{o(\mathscr{W},\mathrm{nd})}(s) = e^{-i\mathscr{H}_{qe}s}\mathscr{H}_D^{o(\mathscr{W},\mathrm{nd})}e^{i\mathscr{H}_{qe}s}$.

The proton-spin cluster will be adequately characterized by two dipolar constants of motion whenever a partition of the dipolar interactions can be found which allows a perturbative approximation of the time evolution operator. In other words, two dipolar quasi-invariants can be defined provided a suitable choice of the interactions involved in $\mathscr{H}_D^{o(\mathscr{S})}$ and $\mathscr{H}_D^{o(\mathscr{W})}$ can be done which enables us to define $\mathscr{H}_D^{o(\mathscr{W},\mathrm{nd})}$ so that $U_{nd}(t_2) \simeq \mathbf{1}$ for $t_2 < t_{qe}$, being t_{qe} a characteristic time for the establishment of the quasi-equilibrium state. Under these conditions the time dependence of the spin density operator of Eq. (11) can be approximated by

$$\rho(t_1,t_2) \simeq U_{qe}(t_2)\rho(t_1,0)U_{qe}^{\dagger}(t_2), \tag{12}$$

where we defined the truncated time evolution operator

$$U_{qe}(t) \equiv e^{-i\mathscr{H}_{qe}t}. \tag{13}$$

The initial density operator can be written as the sum of a diagonal (in blocks) and a non-diagonal term in the eigen-basis of $\mathscr{H}_{qe}$

$$\rho(t_1,0) = \rho_{qe}(t_1) + \rho^{\mathrm{nd}}(t_1), \tag{14}$$

where the quasi-equilibrium term ρ_{qe} does not evolve under $\mathscr{H}_{qe}$, and ρ^{nd} represents the multiple quantum coherences excited by the JB pulse pair [37,38,7,24]. Therefore Eq. (12) is

$$\rho(t_1,t_2) \simeq \rho_{qe}(t_1) + \rho^{\mathrm{nd}}(t_1,t_2), \tag{15}$$

with $\rho^{\mathrm{nd}}(t_1,t_2) = U_{qe}(t_2)\rho^{\mathrm{nd}}(t_1,t_2=0)U_{qe}^{\dagger}(t_2)$. In Eq. (15), ρ_{qe} can be spanned in the quasi-invariants $\mathscr{H}_Z$, $\mathscr{H}_D^{o(\mathscr{S})}$, $\mathscr{H}_D^{o(\mathscr{W},\mathrm{d})}$ and, in principle, other constants of motion [31], and thus $[\rho_{qe}, \mathscr{H}_{qe}] = 0$. For times $t_2 > t_{qe}$ the coherences will have decayed and, in the absence of rf pulses and neglecting spin–lattice relaxation, the state of the spin system becomes time independent. Finally, for times $t_2 \gg t_{qe}$, spin–lattice relaxation causes a time dependence of ρ_{qe} which can be neglected within the timescale treated in this work. Based on previous experimental results [1], we assume that after a waiting time $t_2 > t_{qe}$ and much smaller than the spin–lattice relaxation times, the spin density operator can be written as

$$\rho_{qe}(t_1) = \mathbf{1} - \beta_{\mathscr{S}}(t_1)\mathscr{H}_D^{o(\mathscr{S})} - \beta_{\mathscr{W}}(t_1)\mathscr{H}_D^{o(\mathscr{W},\mathrm{d})}, \tag{16}$$

where the inverse temperatures $\beta_{\mathscr{S}}$ and $\beta_{\mathscr{W}}$ depend only on the preparation time and are defined as

$$\beta_{\mathscr{A}}(t_1) = \frac{Tr\{\rho\mathscr{A}\}}{Tr\{\mathscr{A}^2\}}, \tag{17}$$

with $\mathscr{A} = \mathscr{H}_D^{o(\mathscr{S})}, \mathscr{H}_D^{o(\mathscr{W},\mathrm{d})}$. By properly setting t_1 it is possible to prepare the spin system in each of the dipolar-ordered states [1]; let us call a state of $\mathscr{S}$ order to one which corresponds to $\beta_{\mathscr{W}} \simeq 0$ and $\mathscr{W}$ order to the one with $\beta_{\mathscr{S}} = 0$ [24].

Finally, it is convenient to consider the action of the truncated time evolution operator in more detail. For instance, the evolution of any operator $\mathscr{O}$ under $\mathscr{H}_{qe}$ can be expressed as

$$\mathscr{O}(t) = e^{-i\mathscr{H}_D^{o(\mathscr{W},\mathrm{d})}t}\left\{\mathscr{O} - it[\mathscr{H}_D^{o(\mathscr{S})}, \mathscr{O}] - \frac{t^2}{2}[\mathscr{H}_D^{o(\mathscr{S})}, [\mathscr{H}_D^{o(\mathscr{S})}, \mathscr{O}]] + \cdots\right\}e^{i\mathscr{H}_D^{o(\mathscr{W},\mathrm{d})}t}, \tag{18}$$

according with Eqs. (10) and (13). This expression makes evident that the influence of the $\mathscr{S}$ quasi-invariant on the time evolution depends on the norm of the commutator $\|[\mathscr{H}_D^{o(\mathscr{S})}, \mathscr{O}]\|$ rather than on the relation between the norms of $\mathscr{H}_D^{o(\mathscr{S})}$ and $\mathscr{H}_D^{o(\mathscr{W},\mathrm{d})}$ which are directly determined by the intensity of the dipolar couplings. This implies that a mere comparison of dipolar couplings is not a robust recipe for generating the $\mathscr{S}$ and $\mathscr{W}$ constants of motion in general cases.

3.3. Evolution of the coherences

In order to study the nature of the quasi-equilibrium states ρ_{qe} after the JB pulse pair in LC, we analyse the signals from the usual JB experiment of Fig. 2 (a) and the DQC spectra generated with the pulse sequence by Emid et al. [39], depicted in Fig. 2(b).

The signal after the read pulse of the JB sequence is

$$M(t_1,t)\propto \mathrm{Tr}\{\mathbf{I}_y U_0(t)e^{i(\pi/4)\mathbf{I}_y}\rho_{qe}(t_1)e^{-i(\pi/4)\mathbf{I}_y}U_0^{\dagger}(t)\}, \tag{19}$$

where

$$U_0(t)=e^{-i\mathscr{H}_D^o t}. \tag{20}$$

The hypothesis that the spin state can be represented by a quasi-equilibrium density matrix as Eq. (16) can be tested by studying the signal $M(t_1,t)$ as a function of the preparation time t_1. To further find a suitable partition of the dipolar energy we use the 2D-DQC diagram generated through the experiment of Fig. 2(b) starting from $\mathscr{S}$ order. Then, the state after the second pulse of this sequence is

$$\rho_{qe}=\mathbf{1}-\beta_{\mathscr{S}}\mathscr{H}_D^{o(\mathscr{S})}. \tag{21}$$

The third pulse, represented by $R_3\equiv e^{i(\pi/2)I_{x,y}}$, transforms $\mathscr{H}_D^{o(\mathscr{S})}$ into zero and double quantum coherences [39]:

$$R_3\mathscr{H}_D^{o(\mathscr{S})}R_3^{\dagger}=\mathscr{H}_0^{(\mathscr{S})}\pm\mathscr{H}_2^{(\mathscr{S})}, \tag{22}$$

with

$$\mathscr{H}_0^{(\mathscr{S})}\equiv-\tfrac{1}{2}\mathscr{H}_D^{o(\mathscr{S})}\mathscr{H}_2^{(\mathscr{S})}\equiv\frac{3}{2}\sum_{k<l\in\mathscr{S}}D_{kl}(\mathbf{T}_{2,+2}^{kl}+\mathbf{T}_2^{kl}\quad,-\quad{}_2),$$

where indices k,l run over the spin sites involved in $\mathscr{H}_D^{o(\mathscr{S})}$, and $\mathbf{T}_{2,\pm2}^{kl}=\frac{1}{2}I_{\pm}^k I_{\pm}^l$. The sign before $\mathscr{H}_2$ in Eq. (22) depends on the phase (x or y) of the third pulse, which is used to select the term containing the DQC through a proper phase cycling.

Following the same reasoning that took us from Eqs. (11) to (12), a suitable election of the interactions involved in $\mathscr{H}_D^{o(\mathscr{S})}$, in consistency with the occurrence of two dipolar quasi-constants, allows approximating $U_0(t)\longrightarrow U_{qe}(t)$ instead of Eq. (20). Then, the state after the third pulse is given by $\rho(t_3)\simeq\mathbf{1}-\beta_{\mathscr{S}}e^{-i\mathscr{H}_{qe}t_3}(\mathscr{H}_0^{(\mathscr{S})}\pm\mathscr{H}_2^{(\mathscr{S})})e^{i\mathscr{H}_{qe}t_3}$. The fourth pulse, $R_4=e^{i(\pi/4)I_y}$, transforms the double quantum coherences $\mathscr{H}_2^{(\mathscr{S})}$ and the dipolar order (zero quantum) back into single-quantum coherence, and the observed 2D signal, after the phase cycling that selects the DQC contribution, becomes

$$S(t_3,\tau)\equiv\langle\mathbf{I}_y(t_3,\tau)\rangle\propto\beta_{\mathscr{S}}Tr\{\mathbf{I}_y e^{-i\mathscr{H}_{qe}\tau}R_4e^{-i\mathscr{H}_{qe}t_3}\mathscr{H}_2^{(\mathscr{S})}e^{i\mathscr{H}_{qe}t_3}R_4^{\dagger}e^{i\mathscr{H}_{qe}\tau}\}. \tag{23}$$

Thus, the invariance of the dipolar signals using the complete evolution operator of Eq. (20) or the truncated one of Eq. (13) may serve as a criterion for probing the suitability of the model used to define $\mathscr{H}_D^{o(\mathscr{S})}$ and $\mathscr{H}_D^{o(\mathscr{W},\mathrm{d})}$. It is worth to remark that operators $\mathscr{H}_2^{(\mathscr{S})}$ and $\mathscr{H}_{qe}$ in Eq. (23) are completely determined by the particular election of the interactions involved in $\mathscr{H}_D^{o(\mathscr{S})}$. In this way, the frequency content of the calculated signals and therefore, their agreement with the experiment depends on the suitability of such election. In Section 6 we calculate the NMR signals of Eq. (23) yielded by different models adopted for the spin system.

4. Experiment

The experiments were carried out at 7 T in a Bruker Avance II spectrometer at 27 °C. The sample (Sigma-Aldrich) used is the liquid crystal 5CB in nematic phase with a Zeeman spin–lattice relaxation time, $T_{1Z}=630$ ms and a dipolar $\mathscr{S}$ relaxation time $T_{\mathscr{S}}=310$ ms. The $\pi/2$ pulse width is 2.7 μs, $t_1=26$ μs was used to prepare the maximum $\mathscr{S}$ dipolar order in 5CB [1]. The amount of $\mathscr{W}$ order is negligible for this setting ($t_1=71\pm1$ μs corresponds to the pure $\mathscr{W}$ order condition); a time $t_2=2$ ms was chosen to allow the quasi-equilibrium to establish [24]. Since $t_2\ll T_{1Z}$ there is no Zeeman order, as assumed in Eq. (16).

Fig. 3(a) shows the experimental JB dipolar signals of 5CB for different preparation times t_1. In order to observe the DQC signal only, we used the phase cycle $(x,-x,y,-y)$ for the 3rd pulse and $(x,x,-x,-x)$ for the receiver. A typical signal $S(t_3,\tau)$ of 5CB at $t_3=10$ μs is illustrated in Fig. 2(b). We recorded the evolution of $S(t_3,\tau)$ for increasing times t_3 from 5 to 500 μs in steps of 10 μs and τ in steps of 4 μs. Then for every observation time τ, there is a pseudo-FID $S(t_3)$ which attenuates over a time $t_3\approx100$ μs. The amplitude of these pseudo-FIDs oscillate with τ. We tested the sequence in a sample of powdered adamantane and obtained a pseudo-FID showing the same shape as reported in Ref. [39].

The Fourier transform in t_3 gives the spectrum in the DQC frequency ν_2, $F(\nu_2,\tau)$, as a function of the single-quantum detection time τ. Fig. 4 shows a contour plot of $F(\nu_2,\tau)$ in 5CB measured on-resonance (this frequency corresponds to the on-resonance condition at the isotropic phase). A cut of this plot at $\tau=27$ μs shows unresolved peaks near 15 kHz and also some structure about 6 kHz. This structure manifests all along the τ axis, as illustrated by the cut at $\tau=127$ μs which corresponds to the second maximum of the single-quantum signal and shows a peak near 15 kHz. The frequency–time 2D plot clarifies that the amplitudes of the frequency (ν_2) components vary appreciably with τ. We verified that in contrast with 5CB, powder adamantane (which has only one dipolar quasi-invariant [24]) has a featureless DQC spectra similar to the reported Gaussian shaped one of potassium oxalate monohydrate [14], where the spin system can be well represented by a model of weakly coupled pairs. It is worth mentioning that when irradiated with an offset frequency, $\Delta\nu_0$, the centre of the DQC spectra of both 5CB and adamantane shift to $2\Delta\nu_0$ as expected [39].

5. Numerical calculations and interaction models

Representing the spin system of 5CB molecule implies considering all its 19 protons, however, calculation of the FID of an N spin system entails manipulating a 2^N dimensional Hilbert space. Thus, we restricted our calculations to 10 spins: the 8 aromatic and the two $\alpha-CH_2$ protons, as shown in Fig. 1. The different models used to represent the interaction Hamiltonians needed for calculating the output signals through Eqs. (19) and (23) are shown in Table 2, where the right column shows the subsets of interactions i,j involved in $\mathscr{H}_D^{o(\mathscr{S})}$ of Eq. (5), labelled as in Fig. 1. These models basically differ in the number of neighbours each spin interacts with. Model (i) only includes the strongest dipolar interaction of each spin; that is, a model of weakly interacting strong pairs. Model (ii) incorporates the interaction of $\alpha-CH_2$ protons with the nearest protons of the core and between benzene rings; in this way, all spins (except 8 and 10) take part of two interactions.

The operators used to calculate the NMR signals for the 10-spin system were represented by matrices of dimension 1024×1024, operating under rules of conventional matrix algebra. The angular momentum operators, and therefore all the other operators needed, were first represented in the Zeeman eigen-basis. By diagonalizing the dipolar Hamiltonian of Eq. (2) one finds the matrix which transforms to a convenient basis where the evolution operator is also diagonal. In order to optimize memory usage and speed operations we used sparse matrices, using the criterion that matrix elements α_{kl} satisfying $|\alpha_{kl}|<10^{-6}$ are considered as zero. Consistently, operators are defined by rounding to 5 significant digits. In order to evaluate the effect of such procedure, we compared the results obtained with and without numeric truncation on a 4-spin and 8-spin cluster, and found them indistinguishable.

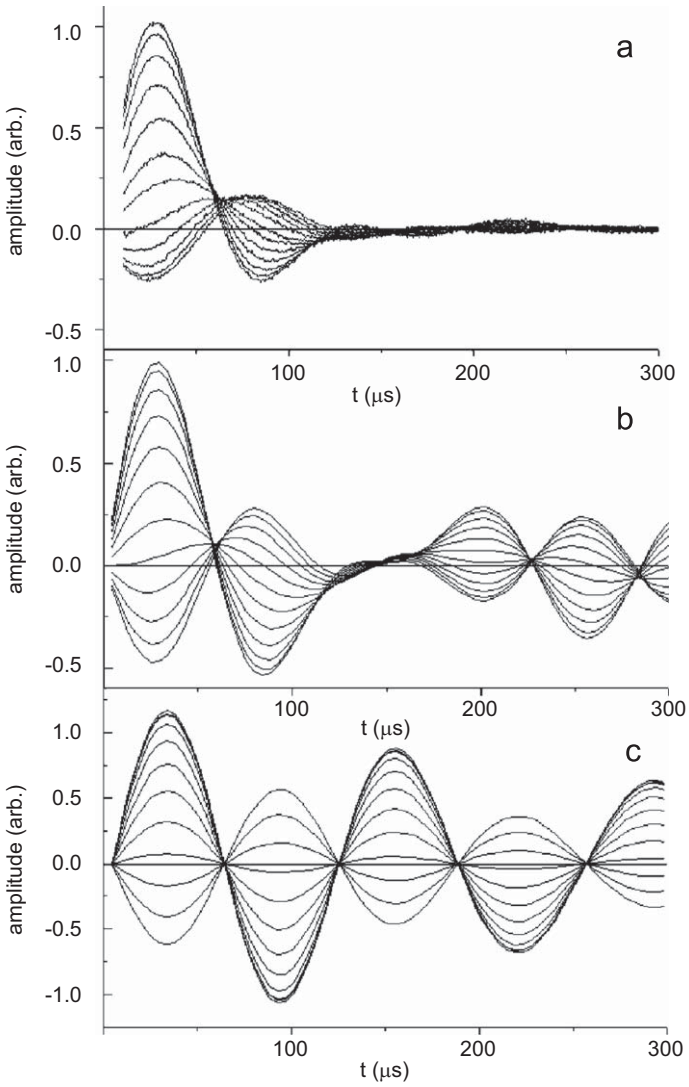

Fig. 3. Dipolar signals after the JB sequence at preparation times from $t_1 = 30$ to 80 μs, (a) experiment, (b) calculated with model (ii) and evolution under $\mathscr{H}_D^o$ and (c) calculated with model (ii) and evolution under $\mathscr{H}_D^{o(\mathscr{S})}$.

6. Results and discussion

6.1. Dipolar single-quantum signals

We first calculate the dipolar NMR signals after the JB sequence of Eq. (19) at different preparation times t_1, with $\mathscr{H}_D^{o(\mathscr{S})}$ according to the models of Table 2. Fig. 3(b) shows that the calculated signals for the 10-spin cluster, provide a good description of the experimental signals of 5CB shown in Fig. 3(a). Notice that no extra attenuation has been added to the calculated signals. Additionally, we found that all the calculated signals have the same qualitative characteristics as the experimental ones, which are, symmetry in the preparation and observation times [1] (not shown), the first maximum of the $\mathscr{S}$ signal occurs around 30 μs and crosses through zero around 70 μs [1]. However, we verified that the signals yielded by different models (i and ii) and different time evolution operators (U_0 or U_{qe}) are not significantly distinct. In contrast, the signals calculated with models (i) and (ii) but using an approximate evolution operator $U_S \equiv e^{-it\mathscr{H}_D^{o(\mathscr{S})}}$ instead of U_0, have a definitely different shape than the experiment for every t_1, as can be seen in Fig. 3(c). Indeed, as commented at the end of Section 3.2, even when $\|\mathscr{H}_D^{o(\mathscr{S})}\| \gg \|\mathscr{H}_D^{o(\mathscr{W})}\|$, which justifies the neglect of non-diagonal components of $\mathscr{H}_D^{o(\mathscr{W})}$, the diagonal part of the weaker couplings cannot be ignored in the time evolution of the coherence. This means that the small terms involved in $\mathscr{H}_D^{o(\mathscr{W},\mathrm{d})}$ play a decisive role in the transfer from the Zeeman order to the dipolar order (especially at longer preparation times), which also determines the complex behaviour of the dipolar signals as a function of t_1 in the JB sequence.

We also verified that there is a good qualitative agreement between the calculated and the experimental dipolar signals of alkyl deuterated 5CB [18] (5CBd_{11}), which has eight protons. In this case we used only the dipolar interactions of Table 1 which involve the aromatic protons and again distinguished two ways of defining $\mathscr{H}_D^{o(\mathscr{S})}$ by including (or not) the inter-ring couplings. Similarly to the 10-spin 5CB case, the SQC signals are not sensible enough to the different models.

The agreement between calculated and experimental signals shown in Fig. 3 confirms that the two-dipolar-quasi-invariants view allows a good description of the experiment [40]. Additionally, it supports our starting assumption of considering only the intramolecular dipolar energy and indicates that there is no need of additional energy terms like long range intermolecular dipole couplings or chemical shift effects to explain the main features of the experimental results. However, the calculation of the outcome of the JB experiment still does not allow a clear qualification of the

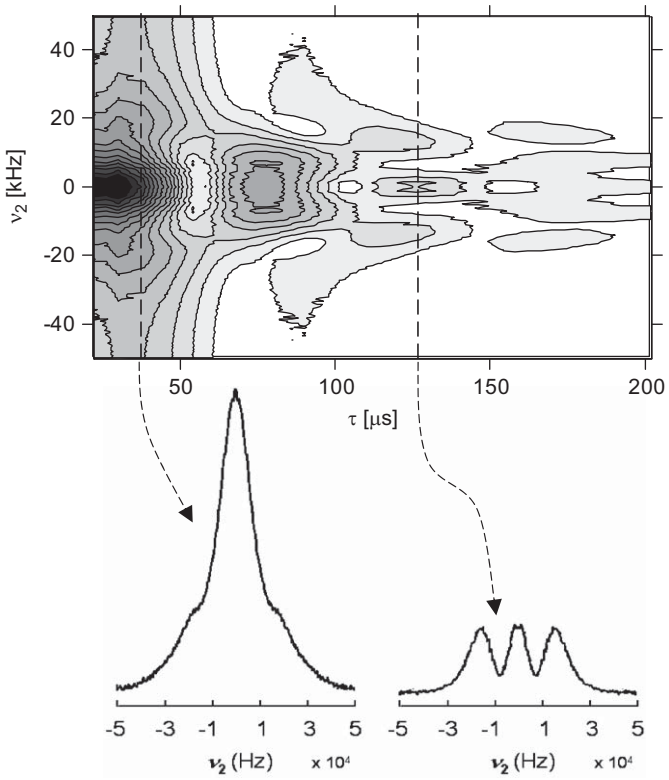

Fig. 4. Contour plot of the experimental on-resonance double quantum coherence amplitude spectra of 5CB as a function of the observation time τ at 27 °C, 300 MHz. Below: cuts at $\tau = 27\,\mu s$ (left) and $\tau = 127\,\mu s$ (right).

Table 2
Sets of interactions used to define $\mathscr{H}_D^{0(\mathscr{S})}$ in the calculations of the dipolar signals and the DQC spectra.

Model	Interactions
(i)	7–8, 9–10, 5–6, 3–4 ,1–2
(ii)	7–8, 9–10, 5–6, 3–4, 1–2, 6–9, 4–7, 1–5, 2–3

different possible ways of partitioning the dipolar energy into strong and weak. Therefore we applied the same test to the 2D signals obtained through the DQC experiment described in the previous section.

6.2. Double quantum spectra

Fig. 5 shows the calculated $F(\nu_2, \tau)$ from Eq. (23), for the 10-spin models. The upper row of Fig. 5 corresponds to model (i) and the lower to model (ii). Plots in the left column were calculated using the time evolution operator of Eq. (20), while the right column corresponds to the truncated one defined in Eq. (13). We represented the additional decoherence due to spins that were not included in the calculation, and other possible sources through a Gaussian decay in both time domains t_3 and τ of frequency width at half height of approximately 3 kHz.

As seen in Figs. 5(a) and (c), both models yield frequency components around 15 kHz for $\tau < 100\,\mu s$, in agreement with the experiment of Fig. 4. However, a drastic difference between models arises when using the truncated time evolution. In Fig. 5(b) the effect of truncation on model (i) is significant since the spectra loose the high frequency structure for every time τ. On the contrary, the effect of truncation on model (ii) is unimportant all along the τ axis as seen by comparing Figs. 5(c) and (d). This is precisely the condition which operators $\mathscr{H}_D^{0(\mathscr{S})}$ and $\mathscr{H}_D^{0(\mathscr{W},\mathrm{d})}$ must fulfil in order to represent satisfactorily a system with two dipolar constants of motion. The 2D analysis of the DQC spectra modulated by the time evolution of the SQC allows the identification of higher frequency components that would otherwise be screened by the width of the lower frequency lines in a 1D experiment. This test provides clear evidence of the effect of truncation, in contrast to the calculations of the single-quantum dipolar signals which are much less sensitive to the different models. It also indicates the suitability of introducing two quasi-invariants associated with different scales of the dipolar energy to describe the spin dynamics in small spin clusters.

In the particular case of weakly coupled pairs, operators $\mathscr{H}_2^{(\mathscr{S})}$ and $\mathscr{H}_D^{0(\mathscr{S})}$ in Eq. (23) commute. Accordingly, the term $\mathscr{H}_D^{0(\mathscr{S})}$ within $\mathscr{H}_{qe}$ in U_{qe}, has no effect on the time evolution of the DQC, which is only driven by $\mathscr{H}_D^{0(\mathscr{W},\mathrm{d})}$, as can be seen from Eq. (18). The

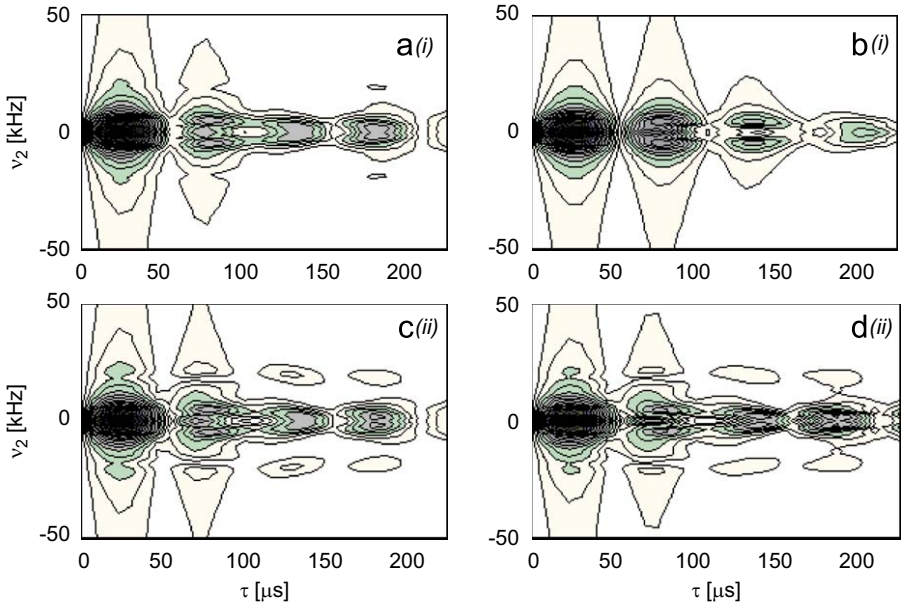

Fig. 5. Contour plots of the calculated double quantum spectra amplitude as a function of the observation time for models (i) and (ii) of the spin system as labelled in Table 2. (a), (b): weakly coupled pairs; (c), (d) correlated spins; (a), (c): evolution with the complete Hamiltonian; (b), (d): evolution with the truncated Hamiltonian. $S_{zz} = 0.75$.

absence of higher frequency structure in Fig. 5(b) is a consequence of this peculiarity of model (i). Conversely, the occurrence of such structure in the DQC spectra is a consequence of the correlated-pairwise-interaction behaviour of the $\mathscr{S}$ quasi-invariant.

The difference between models (i) and (ii) resides in the degree of correlation. In model (ii) the whole cluster becomes a correlated entity. This way of partitioning the dipolar energy explains the main features of the DQC spectra prepared from an $\mathscr{S}$ state as initial condition. The 10-spin set provides enough complexity to account for the main aspects of the 2D frequency–time profile. Nevertheless, the alkyl protons that could not be included in the calculations, possess rather strong residual dipolar couplings of the order of those of the ortho pairs of the benzene rings, and significant intergroup dipolar couplings [41,42]. A subset of the strongest correlated pairwise interactions of the alkyl protons should thereby be also included in $\mathscr{H}_D^{0(\mathscr{S})}$ together with those of model (ii).

It is worth to mention that only two free parameters: the order parameter S_{zz} and the linewidth of the calculated signals were needed to match the characteristic features of the complex pattern of the 2D diagram of Fig. 4. $S_{zz} = 0.75$ was used as the scaling factor in Figs. 3 and 5 in order to agree with the experiment. This value of S_{zz} is somewhat larger than the measured by NMR methods for 27 °C [43]. One could anticipate that considering the 19 protons of the 5CB molecule might correct this difference.

6.3. Conclusions

Summarizing, we can conclude that 5CB molecules admit a partition of the dipolar energy into two orthogonal commuting terms, associated with two energy scales, therefore providing two different spin reservoirs where the original Zeeman order can be stored by means of a Jeener–Broekaert experiment. We confirm that the quasi-equilibrium state after the JB preparation pulse pair can be expanded in terms of two constants of motion which derive from the intramolecular dipolar energy. The results are consistent with the $\mathscr{S}$ reservoir involving all protons of the molecule but only a subset of the dipolar couplings. The fact that $\mathscr{H}_D^{0(\mathscr{S})}$ is better described by a model where all spins are correlated (and not by a weakly interacting-pairs model) is compatible with the multiple-spin correlated nature of the $\mathscr{W}$ reservoir observed in Ref. [24]. Also we find that the small $\mathscr{W}$ energy term plays a significant role in the time evolution of the spin state in spite of the weak interactions involved in this constant of motion.

Some other nematic liquid crystals (5CBd_{11} [18], p-azoxyanisole [4,34] and others) show single-quantum dipolar signals shapes which also change with the preparation time of the JB sequence in similar way. Similitude with 5CB suggests that one might also ascribe this characteristic feature to the occurrence of two constants of motion which derive from the intramolecular dipolar energy to a class of standard thermotropic nematic liquid crystals. The simple experiment applied in this work allows a deep analysis of the DQC spectrum since the modulation provided by the free evolution in the single-quantum time variable enhances the occurrence of DQC frequencies that are screened in a 1D experiment. This kind of DQC frequency vs. SQC time evolution analysis may be applied to study the nature of the different dipolar quasi-invariants in other LC samples [44] or even in solids.

Formally, the quasi-equilibrium state of an N spin system should in principle be written as an expansion of at least 2^N orthogonal terms which commute with the total Hamiltonian, so generalizing Eq. (16) [45]. However, in LC only a small number of invariants can be observed. A theoretical method for generating a subset of additional orthogonal constants of motion starting from the Zeeman and secular dipolar Hamiltonian, which are products of spin operators, was recently presented [31]. Numerical calculations on regularly spaced linear chains of spins 1/2 showed that states of multi-spin order greater than two-spin order would be unobservable in such many-body spin clusters, of typically $N \geq 10$ spins. This characteristic is also present in ordinary solids, like CaF_2, where the Zeeman and the secular dipolar energy are the only observed quasi-invariants [12,7]. For a regular disposition of the spins in the network and N sufficiently large, local field effects would be able to mask the local spin dynamics governed by the nearest neighbours, preventing the existence of two different timescales of the spin dynamics, and therefore of any other constant of motion of multiple-spin character. On the contrary, in a spin cluster like the one of a typical LC molecule, the spin arrangement is far from being regular, thus two scales (at least) of dipolar couplings remain, even for clusters of considerable number of spins, like 5CB. The occurrence of a second, multi-correlated dipolar quasi-invariant, is a consequence of this feature.

Thus, the evolution of the single-quantum coherence under the dipolar energy during the preparation of the JB experiment is characterized by two time scales governed by the $\mathscr{S}$ and $\mathscr{W}$ interactions. In the early t_1 timescale, evolution under the dipolar energy generates bilinear correlations which can then give rise to a two-spin order state represented by $\mathscr{H}_D^{0(\mathscr{S})}$. By other hand, $\mathscr{H}_D^{0(\mathscr{W},\mathrm{d})}$ represents multi-spin order originated in multiple-spin correlations which have grown up over a longer t_1 time scale. This ordered state can be observed by setting the preparation time in the condition $\beta_{\mathscr{S}} = 0$ [1,24]. The occurrence of such spin dynamics is dictated by the topology of the spin distribution in the network, which ultimately determines the characteristics of the multiple-spin-correlation growth [32].

An expression for $\mathscr{H}_D^{0(\mathscr{W},\mathrm{d})}$ in operator form is still unknown, except for the case of an ensemble of dilute pairs like the hydrated crystals [14]. Full decomposition of the signal into spherical tensor components [46] might contribute to a complete determination of this operator for a given LC.

Acknowledgments

This work was supported by Secretaría de Ciencia y Técnica from Universidad Nacional de Córdoba, Consejo Nacional de Investigaciones Científicas y Técnicas (CONICET), Agencia Nacional de Promoción Científica y Técnica (ANPCyT) (Argentina), and the Partner Group with the Max-Planck Institute for Polymer Research, Mainz, Germany. C.J.B. and H.H.S. thank CONICET for financial support.

References

[1] O. Mensio, C.E. González, R.C. Zamar, Phys. Rev. E 71 (2005) 011704.
[2] R.C. Zamar, E. Anoardo, O. Mensio, D.J. Pusiol, S. Becker, F. Noack, J. Chem. Phys. 109 (1998) 1120.
[3] O. Mensio, R.C. Zamar, E. Anoardo, R.H. Acosta, R.Y. Dong, J. Chem. Phys. 123 (2005) 204911.
[4] H.H. Segnorile, L. Barberis, C.E. González, R.C. Zamar, Phys. Rev. E 74 (2006) 051702.
[5] R.C. Zamar, O. Mensio, J. Chem. Phys. 121 (2004) 11927.
[6] T. Charpentier, D. Sakellariou, J. Virlet, F.S. Dzheparov, J.F. Jacquinot, J. Chem. Phys. 127 (2007) 224506.
[7] H. Cho, D. Cory, C. Ramanathan, J. Chem. Phys. 118 (8) (2003) 3686.
[8] S.I. Doronin, E. Feldman, E. Kuznetsova, G.B. Furman, S.D. Goren, Phys. Rev. B 76 (2007) 144405;
S.I. Doronin, E. Feldman, E. Kuznetsova, G.B. Furman, S.D. Goren, Pisma v ZhETF 86 (2007) 26.
[9] B. Furman, S.D. Goren, J. Phys. Condens. Matter 17 (2005) 4501–4509.
[10] C.P. Slichter, W.C. Holton, Phys. Rev. 122 (1961) 1701.
[11] A.G. Anderson, S.R. Hartmann, Phys. Rev. 128 (1962) 2023.
[12] J. Jeener, P. Broekaert, Phys. Rev. 157 (1967) 232.

[13] G.E. Pake, J. Chem. Phys. 16 (1948) 327.
[14] A. Keller, Adv. Magn. Reson. 12 (1988) 183.
[15] H. Eisendrath, W. Stone, J. Jeener, Phys. Rev. B 17 (1978) 47.
[16] H. Eisendrath, J. Jeener, Phys. Rev. B 17 (1978) 54.
[17] E. Dumont, J. Jeener, P. Broekaert, Phys. Rev. B 49 (1994) 6763.
[18] O. Mensio, C.E. González, R.C. Zamar, D.J. Pusiol, R.Y. Dong, Physica B 320 (2002) 416.
[19] P. De Gennes, J. Proust, The Physics of Liquid Crystals, second ed., Oxford University Press, Oxford, 1993.
[20] D.N. Shykind, J. Baum, S.B. Liu, A. Pines, A.N. Garroway, J. Magn. Reson. 76 (1988) 149.
[21] J. Baum, A. Pines, J. Am. Chem. Soc. 108 (1986) 7447.
[22] J. Jensen, Phys. Rev. B 52 (1995) 9611.
[23] K. Lefmann, B. Buras, E.J. Pedersen, E.S. Shabanova, P.A. Thorsen, F.B. Rasmussen, J.P.F. Sellschop, Phys. Rev. B 50 (1994) 15623.
[24] L. Buljubasich, G.A. Monti, R.H. Acosta, C.J. Bonin, C.E. González, R.C. Zamar, J. Chem. Phys. 130 (2009) 024501.
[25] S. Sinton, A. Pines, Chem. Phys. Lett. 76 (1980) 263.
[26] B. Stevensson, A.V. Komolkin, D. Sandström, A. Maliniak, J. Chem. Phys. 114 (2001) 2332.
[27] S.W. Sinton, D.B. Zax, J.B. Murdoch, A. Pines, Mol. Phys. 53 (1984) 333.
[28] There is also agreement between these references and the dipolar couplings calculated in reference [26] for 5CB by molecular dynamics simulation, with the same exception mentioned above. In this case D_{47} and D_{69} have a difference of about 20% with the experiment. Our calculation corresponds to $S_{zz} = 0.54$, to meet with references [25,27]. Since $S_{zz} = 0.5$ in reference [26], a scale factor had to be used in order to compare data.
[29] K. Blum, Density Matrix Theory and Applications, Plenum, New York, 1981.
[30] J. Baum, M. Munowitz, A.N. Garroway, A. Pines, J. Chem. Phys. 83 (1985) 2015.
[31] J.D. Walls, Y. Lin, Solid State Nucl. Magn. Reson. 29 (2006) 22.
[32] H. Cho, T.D. Ladd, J. Baugh, D.G. Cory, C. Ramanathan, Phys. Rev. B 72 (2005) 054427.
[33] In the case of the $\mathscr{W}$-reservoir, the quasi-equilibrium is attained at a much longer time than in the case of $\mathscr{S}$ and the dipolar order of ordinary solids, as shown in Ref. [24]. This feature was attributed to the multiple-spin correlated nature of the $\mathscr{W}$-reservoir.
[34] H. Schmiedel, S. Grande, B. Hillner, Phys. Lett. 91A (1982) 365.
[35] M.H. Levitt, Spin Dynamics, Basics of Nuclear Magnetic Resonance, Wiley, New York, 2001.
[36] R.P. Feynman, Phys. Rev. 84 (1951) 108.
[37] S. Emid, A. Bax, J. Konijnendijk, J. Smidt, A. Pines, Physica 96B (1979) 333.
[38] S. Emid, J. Konijnendijk, J. Smidt, A. Pines, Physica 100B (1980) 215.
[39] S. Emid, J. Smidt, A. Pines, Chem. Phys. Lett. 73 (1980) 496.
[40] We also checked that when assuming only one dipolar quasiinvariant, that is, assuming that $\rho_{qe} = \mathbf{1} - \beta_D \mathscr{H}_D^0$ instead of Eq. (16), the only signals which are similar to the experiment are those calculated under a preparation time near the $\mathscr{S}$ condition.
[41] E. Ciampi, G. De Luca, J.W. Emsley, J. Magn. Reson. 129 (1997) 207.
[42] B. Stevensson, D. Sandstrom, A. Maliniak, J. Chem. Phys. 119 (2003) 2738.
[43] A.V. Komolkin, A. Laaksonen, A. Maliniak, J. Chem. Phys. 101 (1994) 4103.
[44] W.V. Gerasimowicz, A.N. Garroway, J.B. Miller, J. Am. Chem. Soc. 112 (1990) 3726.
[45] D.P. Weitekamp, Adv. Magn. Reson. 11 (1983) 111.
[46] J.D. van Beek, M. Carravetta, G.C. Antonioli, M.H. Levitt, J. Chem. Phys. 122 (2005) 244510.